

INSTABILITY OF LBV-STARS AGAINST RADIAL OSCILLATIONS

2009 Yu. A. Fadeyev¹

Institute of Astronomy, Moscow

In this study we consider the nonlinear radial oscillations exciting in LBV-stars with effective temperatures $1.5 \cdot 10^4 \text{ K} \leq T_{\text{eff}} \leq 3 \cdot 10^4 \text{ K}$, bolometric luminosities $1.2 \cdot 10^6 L_{\odot} \leq L \leq 1.9 \cdot 10^6 L_{\odot}$ and masses $35.7 M_{\odot} \leq M \leq 49.1 M_{\odot}$. Hydrodynamic computations were carried out with initial conditions obtained from evolution sequences of population I stars ($X = 0.7$, $Z = 0.02$) with initial masses in the range $70 M_{\odot} \leq M_{\text{ZAMS}} \leq 90 M_{\odot}$. All models show instability against radial oscillations with amplitude growth time comparable with dynamical time scale of the star. Radial oscillations exist in the form of nonlinear running waves propagating from the boundary of the compact core to the upper boundary of the hydrodynamical model. The velocity amplitude of outer layers is of several hundreds of km/s while the bolometric light amplitude is $\Delta M_{\text{bol}} \leq 0.2$ mag. Stellar oscillations are not driven by the κ -mechanism and are due to the instability of the gas with adiabatic exponent close to the critical value $\Gamma_1 = 4/3$ due to the large contribution of radiation in the total pressure. The range of light variation periods ($6 \text{ day} \leq \Pi \leq 31 \text{ day}$) of hydrodynamical models agrees with periods of microvariability observed in LBV-stars.

Key words: stars – variable and peculiar

PACS numbers: 97.10.Cv; 97.10.Sj; 97.30.Eh

INTRODUCTION

The most luminous ($L \sim 10^6 L_{\odot}$) stars represent a group of luminous blue variables (LBV) which involve such well known objects as η Car, P Cyg, S Dor and the Hubble–Sandage variables in galaxies M31 and M33. All LBV-stars are massive population I stars at the early helium burning stage and their small number is due to the rapid evolutionary movement across the HRD to the higher effective temperatures. LBV-stars are thought to precede the Wolf–Rayet evolutionary stage (Maeder, 1983; Langer et al., 1994) though it is not excepted that they might also be the supernova progenitors (Gal–Yam et al., 2007; Trundle et al., 2008).

Photometric variability of LBV-stars can be divided into three distinct types depending on the characteristic time scale (Lamers, 1987; Leitherer et al., 1992). In variability of the first type (giant eruptions) the bolometric luminosity increases by several magnitudes and the mass of the ejected material is as high as $\sim M_{\odot}$ (Humphreys & Davidson, 1994). The energy of the giant eruption can be so high that the LBV-star becomes the SN-impostor (Smith et al.,

¹e-mail: fadeyev@inasan.ru

2009). There are known two giant eruption events in the Galaxy. One of them was P Cyg in the early XVII century (de Groot, 1988) and another was η Car in the middle of XIX century (van Genderen, 1984; Frew, 2004), so that the time scale of giant eruptions is thought to be of the order of $\gtrsim 10^2$ yr. In variability of the second type (S Dor type) with time scale of ~ 10 yr the bolometric light seems do not change, whereas the visual light changes by about 2 mag (van Genderen, 2001). During the absence of S Dor type variability one can observe the cyclic light variations (microvariability) with amplitude of ≤ 0.2 mag and characteristic time ranging from one to several dozens of day.

The origin of the both giant eruptions and S Dor variability remains still unclear and only microvariations are interpreted in terms of stellar pulsations (van Genderen, 1989). This assumption is supported by the linear theory of stellar pulsation (Glatzel & Kiriakidis, 1993; Kiriakidis et al., 1993; Dziembowski & Slawinska, 2005) which predicts that outer layers of LBV–stars are unstable against radial oscillations. This fact seems to be of great importance because observational estimates of microvarion periods can provide us with independent method of mass determination.

The goal of the present study is to consider nonlinear radial stellar oscillations as a cause of microvariability in LBV–stars. Hydrodynamic modeling of this phenomenon is too complicated because of the large amplitude oscillations exciting at the boundary of the dynamical instability, so that only two reports on this item have been published by now (Dorfi et al., 2000; Dorfi & Gautschy, 2002). Below we present the results of hydrodynamic calculations of radial oscillations in LBV–stars with effective temperatures $1.5 \cdot 10^4 \text{ K} \leq T_{\text{eff}} \leq 3 \cdot 10^4 \text{ K}$ and luminosities $1.2 \cdot 10^6 L_{\odot} \leq L \leq 1.9 \cdot 10^6 L_{\odot}$. Initial conditions for the Cauchy problem of the equations of radiation hydrodynamics were taken from the stellar evolution calculations for population I stars ($X = 0.7$, $Z = 0.02$) with initial masses $70M_{\odot} \leq M_{\text{ZAMS}} \leq 90M_{\odot}$. This paper continues our earlier studies of nonlinear radial oscillations in the massive helium–burning stars (Fadeyev, 2007; 2008a; 2008b) where the computational methods are described in more detail.

EVOLUTIONARY MODELS

In the present study the stellar evolution during the hydrogen core burning was calculated with mass loss rates \dot{M} by Vink et al. (2000, 2001) that are based on the stellar wind models with multiple photon scattering and that are in a good agreement with observations of O and B stars. Comparison with our previous calculations (Fadeyev, 2007, 2008a, 2008b) shows that application of the formula by Nieuwenhuijzen and de Jager (1990) for the hydrogen burning phase leads to much higher (by a factor of $\lesssim 20$) mass loss rates and, therefore, to substantially smaller stellar mass and luminosity at the core hydrogen exhaustion. For example, evolution calculation for the star $M_{\text{ZAMS}} = 80M_{\odot}$ up to the central hydrogen abundance $X_c = 10^{-5}$ gives

the stellar mass and luminosity $M = 43.6M_{\odot}$ and $L = 1.27 \cdot 10^6 L_{\odot}$ with mass loss rates by Nieuwenhuijzen and de Jager (1990), whereas from calculations with mass loss rates by Vink et al. (2000, 2001) the mass and luminosity are $M = 50.9M_{\odot}$ and $L = 1.55 \cdot 10^6 L_{\odot}$.

The formulae for \dot{M} by Vink et al. (2000, 2001) become inapplicable after the core hydrogen exhaustion and following Vazquez et al., (2007) the mass loss rates at later evolutionary stages were calculated according to Nieuwenhuijzen and de Jager (1990). During the helium core burning when the effective temperature rises above $T_{\text{eff}} = 10^4$ K the mass loss rates were calculated according to Nugis and Lamers (2000).

Fig. 1 displays the HRD with several LBV–stars with luminosities and effective temperatures from de Jager (1998). On the same figure are shown the parts of evolutionary tracks with initial masses $M_{\text{ZAMS}} = 70M_{\odot}$ and $M_{\text{ZAMS}} = 90M_{\odot}$. The tracks cross the HR–diagram from the right to the left and labels at the tracks give the central helium mass fraction Y_c . Within the displayed parts of the tracks the central temperature T_c and the central gas density ρ_c change negligibly. For all models $T_c \approx 2.15 \cdot 10^8$ K while the central gas density ranges within $\rho_c \approx 250 \text{ cm}^3/\text{g}$ for $M_{\text{ZAMS}} = 90M_{\odot}$ and $\rho_c \approx 300 \text{ cm}^3/\text{g}$ for $M_{\text{ZAMS}} = 70M_{\odot}$.

For $M_{\text{ZAMS}} = 70M_{\odot}$ the time needed to cross the effective temperature range $1.5 \cdot 10^4 \text{ K} \leq T_{\text{eff}} \leq 5 \cdot 10^4 \text{ K}$ is $\approx 8 \cdot 10^3$ yr and the stellar mass decreases from $36M_{\odot}$ to $31M_{\odot}$. For $M_{\text{ZAMS}} = 90M_{\odot}$ the evolution time within the same effective temperature range is $\approx 5 \cdot 10^4$ yr and the stellar mass decreases from $49M_{\odot}$ to $36M_{\odot}$. Vink and de Koter (2003) evaluated the mass of AG Car as $M \approx 35M_{\odot}$. Bearing in mind existing uncertainties in estimates of the luminosities of LBV–stars one may conclude that evolutionary sequences computed in the present study are in a good agreement with observations.

HYDRODYNAMIC MODELS

Some evolutionary stellar models corresponding to the early helium core burning were used as initial conditions in hydrodynamic computations of the self–exciting radial stellar oscillations. Main parameters of the hydrostatically equilibrium models are given in the table, where R is the equilibrium radius of photosphere. For effective temperatures $1.5 \cdot 10^4 \text{ K} \leq T_{\text{eff}} \leq 3 \cdot 10^4 \text{ K}$ the mass of the envelope surrounding the compact core is almost negligible ($M_{\text{env}} \lesssim 10^{-5}M$) and the mean molecular weight of the stellar material in the envelope does not depend on the radius r . Thus, the surface mass fractions of hydrogen X_s and helium Y_s given in the table are the same for all mass zones of hydrodynamical models.

Outer layers of hydrostatically equilibrium LBV–stars are very close to the boundary of dynamical instability due to the large radiation pressure, so that approximation errors of finite–difference equations can lead to expansion of outer mass zones with velocity higher than the local escape velocity. In such a case the oscillations can be computed only within a too short time

interval because when the radius of the upper boundary becomes about several dozen times its initial value the iteration solution of implicit difference equations do not converge. To overcome this obstacle one should diminish approximation errors of the difference equations. After a number of test computations it was found that the appropriate solution can be obtained for the number of mass zones ranging within $10^3 \leq N \leq 3 \cdot 10^3$. In all hydrodynamic models the size of the mass interval decreases to the inner boundary in order to provide enough approximation at the core boundary where the gas temperature, pressure and density undergo the sharp rise to the center.

It is assumed that the radius and luminosity at the inner boundary remain constant, that is $\partial r_0/\partial t = \partial L_0/\partial t = 0$. Determination of the inner radius r_0 needs the compromise between the demands of accuracy and the time step limitations imposed by the Courant stability criterion. Choosing the location of the inner boundary and the distribution of mass zones we tried to satisfy the condition that the integration time step is $\Delta t \sim 10^{-5} t_{\text{dyn}}$, where $t_{\text{dyn}} = (R^3/GM)^{1/2}$ is the dynamical time scale of the star and G is the Newtonian constant of gravitation. Thus, the ratio of the radius of the inner boundary to the equilibrium radius of photosphere is $0.01 \leq r_0/R \leq 0.05$. The gas temperature at the inner boundary ranges within $5 \cdot 10^5 \text{ K} \leq T_0 \leq 10^6 \text{ K}$, so that therminuclear energy sources can be ignored.

Hydrodynamic computations with the large number of mass zones are time consuming but they allowed us to obtain the solution of the equations of hydrodynamics within time intervals as long as 10^4 day and to apply the discrete Fourier transform for determination of the mean period Π of radial stellar pulsation. It should be noted however that due to irregular dynamical behaviour the expansion velocity of the upper boundary sometimes exceeded the local escape velocity. In such cases one or a few mass zones excluded from the model and calculations were continued with the smaller number of mass zones N .

All the models of LBV–stars considered in the present study were found to be unstable against radial oscillations, the amplitude growth time being comparable with dynamical time scale t_{dyn} . The amplitude growth ceases at the amplitude $\delta r_s \sim R$, so that radial oscillations of LBV–stars are strongly nonlinear. The nonlinear radial oscillations are illustrated in Fig. 2(a) and Fig. 2(b) where the temporal dependences of the velocity U_s and the radius r_s of the upper boundary are shown for the model $M_{\text{ZAMS}} = 70M_{\odot}$, $T_{\text{eff}} = 3 \cdot 10^4 \text{ K}$.

Notwithstanding the large amplitude of the radial displacement the amplitude of light changes is $\leq 0.2 \text{ mag}$. Here one should note that the rapid light variations (for the model in Fig. 2 with characteristic time $\lesssim 1 \text{ day}$) are due to the discrete nature of the hydrodynamical model and therefore they are not connected with stellar pulsation.

In contrast to the most classical radially pulsating stars where nonlinear effects become important in the outer layers (e.g., W Vir and Mira–type variables) radial oscillations of LBV–stars are nonlinear within the entire envelope. This is due to the small pressure gradient and

approximately constant gas density between the core boundary and the photosphere. Large amplitude oscillations in different layers of the pulsating envelope are shown in Fig. 3 where plots of the gas flow velocity U are given for several mass zones of the hydrodynamical model. For the sake of convenience the plots are arbitrarily shifted along the vertical axis. The lowest plot in Fig. 3 corresponds to the layers with the mean radius $r < 0.1R$.

The main parameter of the radially pulsating star is the pulsation period Π but calculation of this quantity for hydrodynamic models of LBV–stars is complicated not only due to irregular oscillations. The problem is that the most of the mass is confined inside the compact core and the mass of the envelope surrounding the core is $M_{\text{env}} \lesssim 10^{-5}M$, whereas its extension is about 0.9 of the stellar radius. Because of the low gas density and the small sound speed the characteristic motion time of the envelope layers is significantly longer than that of the core boundary, so that radial oscillations of LBV–stars are rather the nonlinear running waves propagating from the inner core to the stellar surface. Effects of running waves are illustrated in Fig. 4(a), where three plots of the gas flow velocity U are shown as a function of the Lagrangean coordinate measured from the inner boundary. The expansion of inner layers occurs approximately at $t = t_1$ and $t = t_2$ but displacement of the running wave during the time interval $t_2 - t_1$ is significantly less than the stellar radius. Thus, the running wave reaches the upper boundary during several oscillation periods of inner layers. Dependence of the oscillation period on the spatial coordinate is clearly seen from velocity plots corresponding to different depths inside the envelope (Fig. 3).

The bolometric radiation flux from the upper boundary depends on the contribution of layers at different depths with different oscillation periods. That is why light variations rather weakly correlate with variations of the upper boundary velocity (see Fig. 2). The pulsation period calculated from the discrete Fourier transform of the kinetic energy E_K of the pulsating envelope is always longer than that evaluated from the light curve. This is due to the fact that the most of the kinetic energy is contributed by outer layers, whereas the light variations depend on deeper layers with shorter periods. The typical Fourier spectra of the kinetic energy $S(E_K)$ and bolometric light $S(\Delta M_{\text{bol}})$ are shown in Fig. 5 for the model $M_{\text{ZAMS}} = 80M_{\odot}$, $T_{\text{eff}} = 2 \cdot 10^4$ K. The mean period of variations of the kinetic energy is $\Pi(E_K) = 51.2$ day while the mean light period is $\Pi = 16.6$ day.

Last two columns of the table give the mean periods of light changes Π and corresponding pulsation constants Q . Here one should bear in mind that in contrast to radial pulsations in the form of standing waves the pulsation constants of LBV–stars cannot be considered as their mechanical characteristics.

The sharp increase of the luminosity L_r at the front of the running wave propagating to the upper boundary (see Fig. 4) is the principal cause of the change of radiation flux emerging from the upper boundary. Thus, the light variations of LBV–stars are due to dissipation of the

kinetic energy of running waves rather than due to κ -mechanism. Indeed, modulation of the radiation flux by κ -mechanism can arise in the vicinity of Z-bump ($T \approx 2 \cdot 10^5$ K) but in LBV-stars these layers are at the boundary of the compact core, so that their mass is too small for driving the pulsational instability. For some models we carried out hydrodynamical calculations with different location of the inner boundary and found that models with temperature at the inner boundary $T \sim 10^5$ K demonstrate instability similar to that obtained for models with deeper inner boundary locating below the Z-bump. Therefore, the pulsational instability is due to the fact that the adiabatic exponent within the envelope is close to the critical value $\Gamma_1 = 4/3$. The inefficiency of the κ -mechanism in LBV-stars was considered in the framework of the linear theory by Kiriakidis et al. (1993).

CONCLUSION

In the present study we computed the hydrodynamical models of radially oscillating LBV-stars with effective temperatures $1.5 \cdot 10^4$ K $\leq T_{\text{eff}} \leq 3 \cdot 10^4$ K and this allows us to conclude that microvariability is most probably due to radial oscillations. The κ -mechanism is not responsible for pulsational instability and oscillations appear is due thermodynamical properties of the stellar material with adiabatic exponent close to its critical value $\Gamma_1 = 4/3$. Strongly nonadiabatic oscillations prevent the development of the dynamical instability due to large radiative losses accompanying the motion of the gas.

Nonlinear radial oscillations of LBV-stars exist in the form of nonlinear running waves propagating from the boundary of the compact core to the stellar surface, the amplitude of radial velocity variations being as large as several hundred km/s. The amplitude of theoretical bolometric light curve is ($\Delta M_{\text{bol}} \leq 0.2$ mag) seems to be overestimated due to limited spatial resolution of hydrodynamical models.

Mean periods estimated from hydrodynamical models (6 day $\leq \Pi \leq 31$ day) are in agreement with observations. For example, observational estimates of microvarion periods are as follows: $\Pi(\text{P Cyg}) \approx 17.3$ day (de Groot et al., 2001), $\Pi(\text{B416 M33}) \approx 8.26$ day (Shemer et al., 2000), 20 day $\leq \Pi(\text{v532 M31}) \leq 30$ day (Sholukhova et al., 2002), 25.7 day $\leq \Pi(\zeta^1 \text{ Sco}) \leq 32$ day (Sterken et al., 1997). The only exception is η Car but its too long period of $\Pi = 58.58$ day (Sterken et al., 1996) is rather due to extremely high luminosity ($L \sim 5 \cdot 10^6 L_{\odot}$) of this star.

REFERENCES

1. G.A. Vazquez, C. Leitherer, et al., *Astrophys. J.*, **663**, 995 (2007).
2. J.S. Vink, A. de Koter, *IAUS*, **212**, 259 (2003).
3. J.S. Vink, A. de Koter, H.J.G.L.M. Lamers, *Astron.Astrophys.*, **362**, 295 (2000)
4. J.S. Vink, A. de Koter, H.J.G.L.M. Lamers, *Astron.Astrophys.*, **369**, 574 (2001)
5. A. Gal-Yam, D.C. Leonard, D.B. Fox, et al., *Astrophys. J.*, **656**, 372 (2007).
6. A.M. van Genderen, *Astron.Astrophys.*, **208**, 135 (1989)
7. A.M. van Genderen, *Astron. Astrophys.*, **366**, 508 (2001).
8. A.M. van Genderen, P.S. Thé, *Space Sci. Rev.*, **39**, 317 (1984).
9. W. Glatzel, M. Kiriakidis, *MNRAS*, **263**, 375 (1993).
10. M. de Groot, *IrAJ*, **18**, 163 (1988).
11. M. de Groot, C. Sterken, A.M. van Genderen, *Astron. Astrophys.*, **376**, 224 (2001).
12. W. Dziembowski, J. Slawinska, *Acta Astron.*, **55**, 195 (2005).
13. E.A. Dorfi, M.U. Feuchtinger, A. Gautschy, *ASP Conf. Ser.*, **203**, 109 (2000).
14. E.A. Dorfi, A. Gautschy, *Comm. in Asteroseismology*, **141**, 57 (2002).
15. M. Kiriakidis, K.J. Fricke, W. Glatzel, *MNRAS*, **264**, 50 (1993).
16. Lamers, H.J.G.L.M. 1987, in *Instabilities in Luminous Early-Type Stars*, ed. H.J.G.L.M. Lamers, and C.W.H. de Loore (Dordrecht: Reidel), p. 99.
17. N. Langer, W.-R. Hamann, M. Lennon, et al., *Astron. Astrophys.*, **290**, 819 (1994).
18. C. Leitherer, N.A. Damineli, W. Schmutz, *ASP Conf. Ser.*, **22**, 366 (1992)
19. A. Maeder, *Astron. Astrophys.*, **120**, 113 (1983).
20. N. Nugis, H. J. G. L. M. Lamers, *Astron. Astrophys.*, **360**, 227 (2000).
21. H. Nieuwenhuijzen and C. de Jager, *Astron.Astrophys.*, **231**, 134 (1990).
22. N., Smith, M. Ganeshalingam, R. Chornock, et al., *Astrophys. J.*, **697**, L49 (2009).
23. C. Sterken, M.J.H. de Groot, A.M. van Genderen, *Astron. Astrophys. Suppl. Ser.*, **116**, 9 (1996).

24. C. Sterken, M.J.H. de Groot, A.M. van Genderen, *Astron. Astrophys.*, **326**, 640 (1997).
25. C. Trundle, R. Kotak, J.S. Vink, et al., *Astron. Astrophys.*, **483**, L47 (2008).
26. Yu.A. Fadeyev, *Ast.L.*, **33**, 645 (2007).
27. Yu.A. Fadeyev, *Ast.Rep.*, **52**, 645 (2008a).
28. Yu.A. Fadeyev, *Ast.L.*, **34**, 772 (2008b).
29. D.J. Frew, *J. Astron. Data*, **10**, 6 (2004).
30. R.M. Humphreys, K. Davidson, *PASP*, **106**, 1025 (1994).
31. O. Shemmer, E.M. Leibowitz, P. Szkody, *MNRAS*, **311**, 698 (2000).
32. O. Sholukhova, A. Zharova, S. Fabrika, D. Malinovskii, *ASP Conf. Ser.*, **259**, 522 (2002).
33. C. de Jager, *Astron. Astrophys. Rev.*, **8**, 145 (1998).

Table 1: Models of LBV-stars.

$M_{\text{ZAMS}}/M_{\odot}$	$T_{\text{eff}}, 10^3 \text{ K}$	L/L_{\odot}	M/M_{\odot}	R/R_{\odot}	X_{s}	Y_{s}	$\Pi, \text{ day}$	$Q, \text{ day}$
70	15	$1.24 \cdot 10^6$	36.02	165	0.23	0.75	28	0.079
	20	$1.24 \cdot 10^6$	35.82	93	0.21	0.77	16	0.107
	30	$1.24 \cdot 10^6$	35.68	41	0.16	0.82	6	0.135
80	15	$1.63 \cdot 10^6$	42.48	190	0.12	0.86	30	0.074
	20	$1.60 \cdot 10^6$	42.33	105	0.12	0.86	17	0.102
	25	$1.56 \cdot 10^6$	42.13	67	0.12	0.86	10	0.119
	30	$1.51 \cdot 10^6$	41.84	46	0.11	0.87	6	0.126
90	15	$1.90 \cdot 10^6$	49.06	205	0.11	0.87	31	0.074
	20	$1.86 \cdot 10^6$	48.80	105	0.11	0.87	16	0.092
	25	$1.80 \cdot 10^6$	47.81	72	0.11	0.87	12	0.137
	30	$1.78 \cdot 10^6$	47.18	50	0.09	0.89	7	0.137

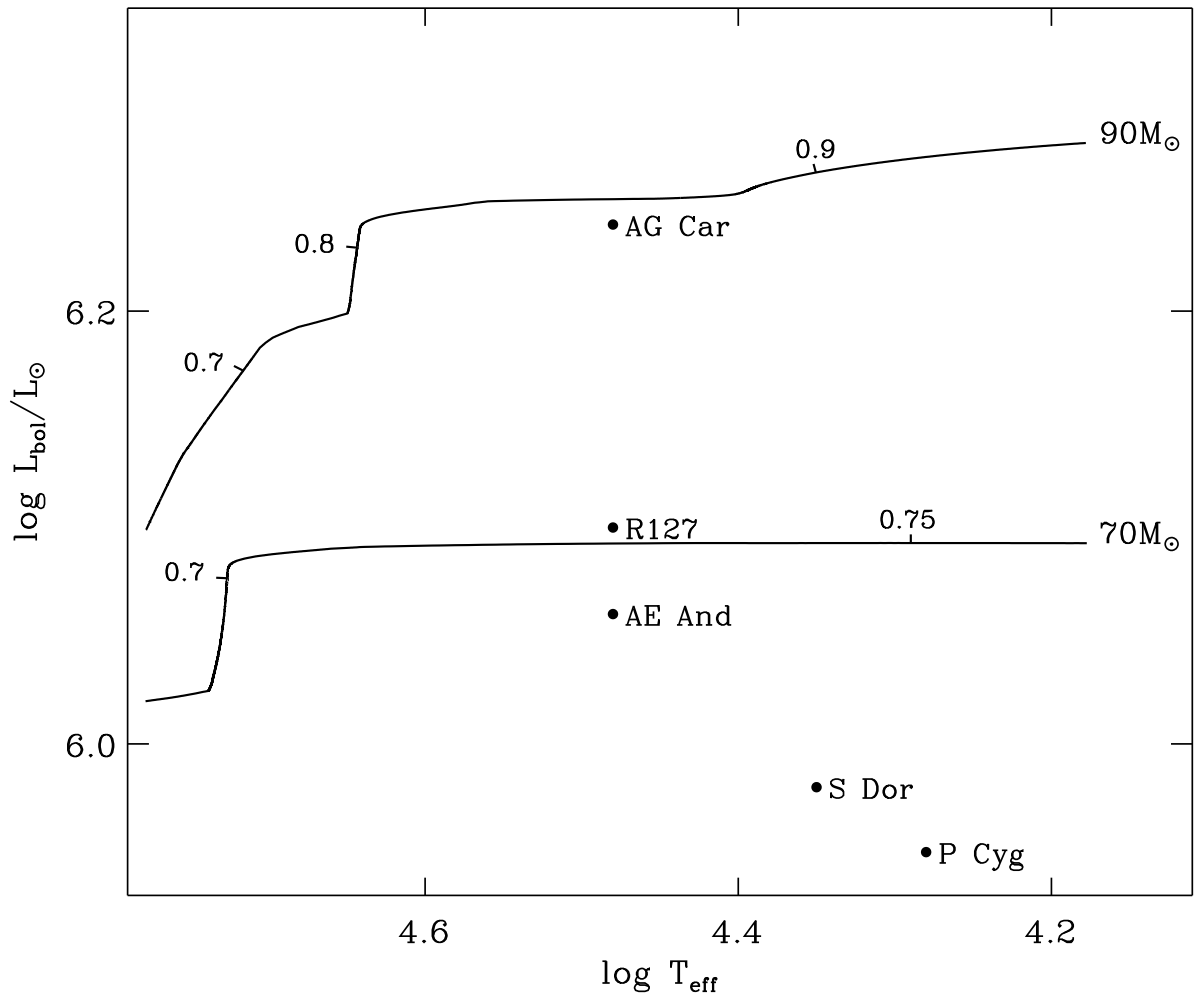


Figure 1: LBV-stars on the HRD (according to de Jager (1998)) and parts of the evolutionary tracks $M_{\text{ZAMS}} = 70M_{\odot}$ and $M_{\text{ZAMS}} = 90M_{\odot}$. Attached at the curves are the values of the central helium abundance Y_c .

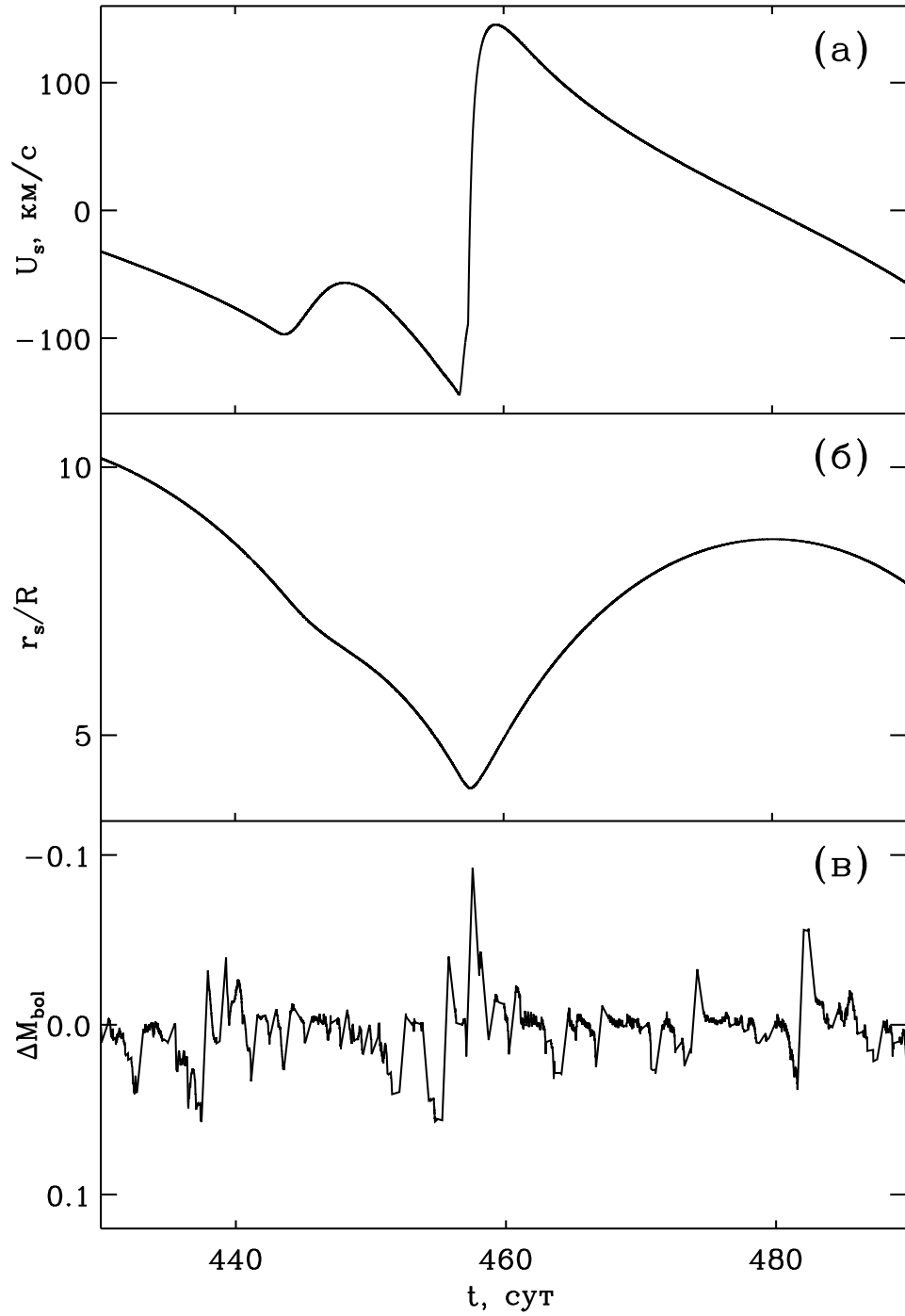


Figure 2: Hydrodynamical model $M_{\text{ZAMS}} = 70M_{\odot}$, $T_{\text{eff}} = 3 \cdot 10^4$ K ($M = 35.7M_{\odot}$, $L = 1.2 \cdot 10^6 L_{\odot}$). (a) – Gas flow velocity at the upper boundary of the model U_s ; (b) – the radius of the upper boundary r_s in units of the equilibrium radius of photosphere; (c) – bolometric light ΔM_{bol} .

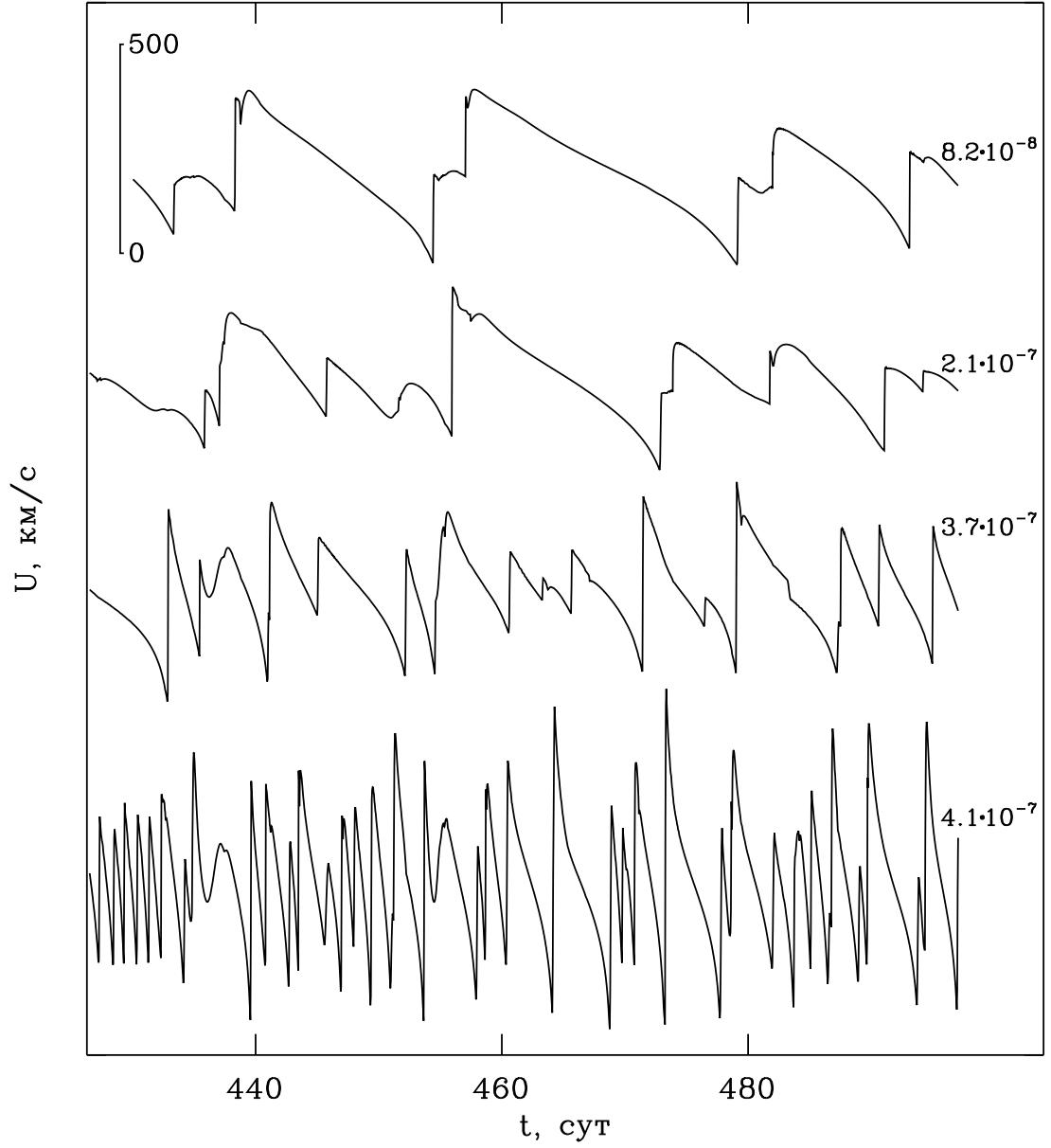


Figure 3: The gas flow velocity U in some mass zones of the same model as in Fig. 2. The plots are arbitrarily shifted along the vertical axis. Attached at the plots is the Lagrangean coordinate $1 - M_r/M$.

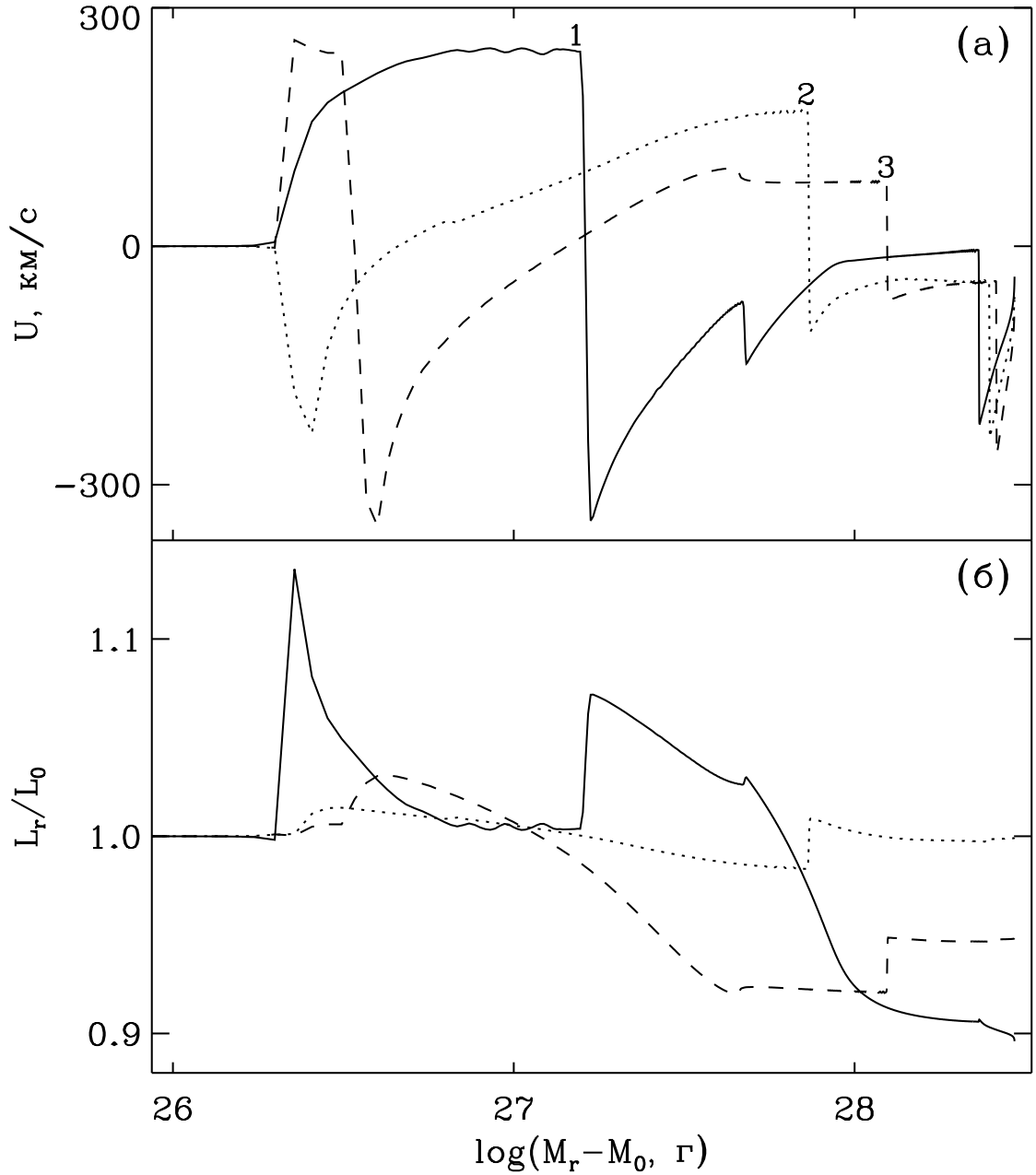


Figure 4: (a) – The gas flow velocity U ; (b) – the luminosity L_r in units of the equilibrium luminosity L_0 as a function of the Lagrangean coordinate measured from the inner boundary. The hydrodynamics model is the same as in Fig 2 and Fig. 3. In solid, dotted and slashed lines are shown the plots for t_1 , t_2 and t_3 .

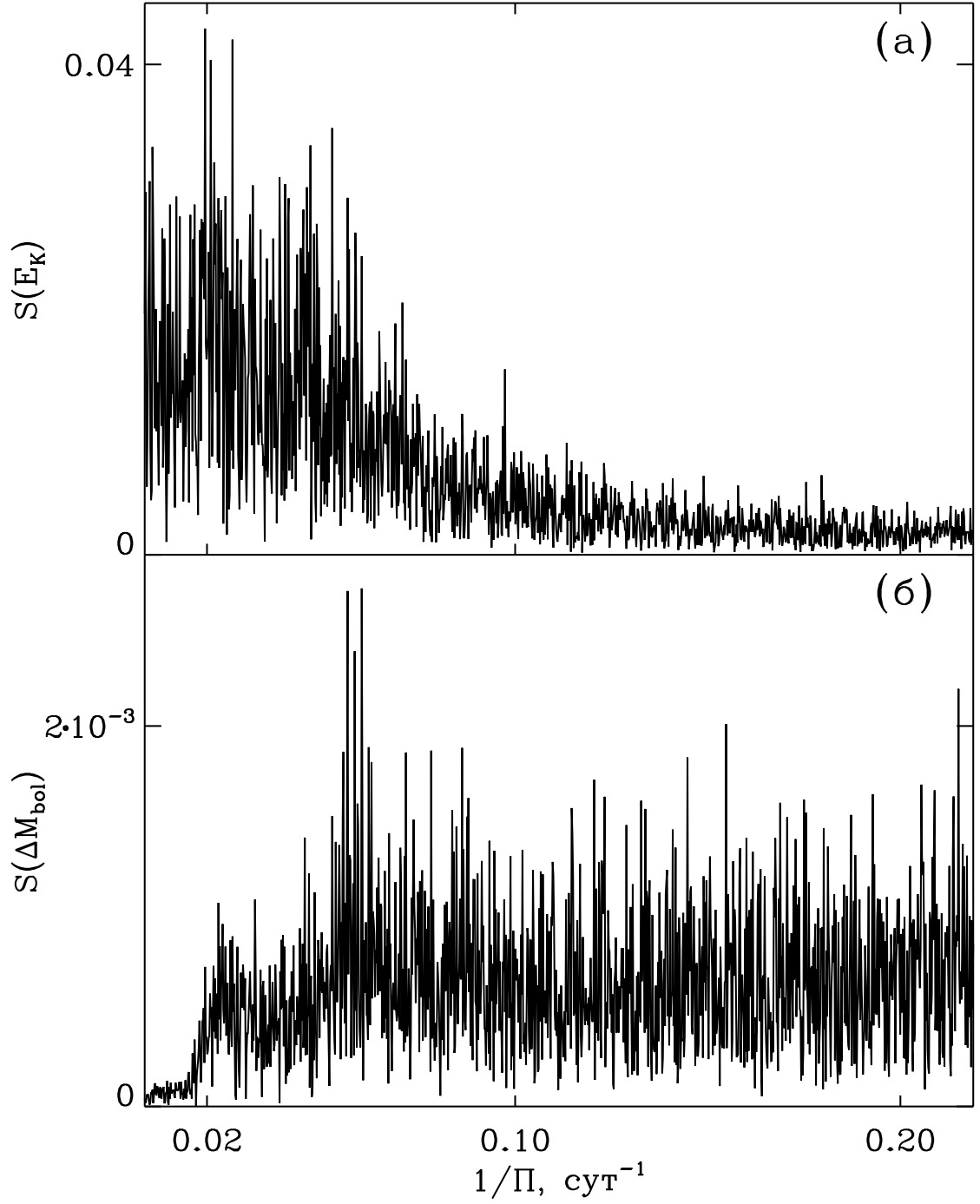


Figure 5: The hydrodynamical model $M_{\text{ZAMS}} = 80M_{\odot}$, $T_{\text{eff}} = 2 \cdot 10^4 \text{ K}$ ($M = 42.3M_{\odot}$, $L = 1.6 \cdot 10^6 L_{\odot}$). (a) – The Fourier spectrum of the kinetic energy of pulsating envelope $S(E_K)$; (b) – the Fourier spectrum of the bolometric light $S(\Delta M_{\text{bol}})$.